Journal of Controlled Release 146 (2010) 400–408

Contents lists available at ScienceDirect

Journal of Controlled Release

journal homepage: www.elsevier.com/locate/jconrel

Thermosensitive hydrogel-containing polymersomes for controlled drug delivery

Jung Seok Lee [a], Wei Zhou [a], Fenghua Meng [a,c], Dianwen Zhang [b], Cees Otto [b], Jan Feijen [a,*]

[a] Department of Polymer Chemistry and Biomaterials, Institute for Biomedical Technology and Technical Medicine, MIRA, Faculty of Science and Technology, University of Twente, Enschede, The Netherlands
[b] MESA+ Institute for Nanotechnology, Biophysical Engineering Group, University of Twente, Enschede, The Netherlands
[c] Biomedical Polymers Laboratory, and Key Laboratory of Organic Synthesis of Jiangsu Province, College of Chemistry, Chemical Engineering and Materials Science, Soochow University, Suzhou, 215123, People's Republic of China

ARTICLE INFO

Article history:
Received 12 November 2009
Accepted 1 June 2010
Available online 8 June 2010

Keywords:
Poly(ethylene glycol)-b-poly(*D,L*-lactide)
Poly(*N*-isopropylacrylamide)
Biodegradable polymersomes
Thermosensitive hydrogel
Controlled drug delivery

ABSTRACT

PNIPAAm-containing polymersomes (N/Ps) were prepared by injecting a solution of poly(ethylene glycol)-b-poly(*D,L*-lactide) (mPEG-PDLLA) and poly(*N*-isopropylacrylamide) (PNIPAAm) in THF into water to incorporate PNIPAAm into polymersomes (Ps). At 37 °C, hydrogel-containing Ps (Hs, hydrosomes) with an average diameter of 127 nm as measured with dynamic light scattering (DLS) were obtained which may be used as potential novel carriers for anticancer drugs and proteins. Dual-labeled N/Ps (FITC-N/RB-Ps) were prepared analogously using rhodamine B tagged mPEG-PDLLA (mPEG-PDLLA-RB) and fluorescein isothiocyanate labeled PNIPAAm (FITC-N). The co-localization of RB labeled Ps (RB-Ps) and FITC-N in RB-Ps was shown by dual fluorescence CLSM. Fluorescence correlation spectroscopy (FCS) and fluorescence anisotropy (FA) measurements with these systems gave further evidence for the colocalization of PNIPAAm and Ps. Micron-sized giant Ps with a diameter of 5–10 μm containing FITC-N were prepared using $CHCl_3$ as the organic phase. The presence of FITC-N in these giant Ps as well as the phase separation of the internal FITC-N solution above the lower critical solution temperature (LCST) was also shown by CLSM. The release of fluorescein isothiocyanate tagged dextran (FD, FITC-dextran, Mw 4000 g/mol) from Hs revealed that in the presence of the hydrogel at 37 °C a more sustained release of FD (up to 30 days) with a low initial burst effect was obtained as compared to the release from bare Ps.

1. Introduction

Although a large number of drug delivery systems has been designed during the past few decades, there is still a need for further reduction of side effects, more convenient methods of administration and an improvement of patient compliance [1,2]. Some of these requirements can be achieved by using injectable nanocarrier systems, providing a temporal modulated drug release for predefined periods as well as a spatial drug distribution control in the body [3].

Polymersomes (Ps), synthetic supramolecular-structures similar to liposomes but composed of amphiphilic block copolymers instead of lipids [4], have attracted a lot of attention among the various nanocarrier systems due to their outstanding stability and relatively long circulation times [5,6]. Long circulation times of Ps can be accomplished by applying a poly(ethylene glycol) (PEG) layer on the surface of the Ps as previously reported by Lee et al. and Photos et al. [6,7]. The presence of PEG reduces protein adsorption onto the Ps [8,9], which is caused by the relatively low interfacial energy of the water containing PEG layer and water, and the steric hindrance provided by the PEG molecules [10–12].

Drug delivery from Ps can be controlled by varying the permeability of the bi-layer. Bermudez et al. and Ahmed et al. prepared Ps based on block copolymers such as PEG-poly(butadiene) (PEG-PBD), PEG-poly(ethylethylene) (PEG-PEE), PEG-poly(lactic acid) (PEG-PLA) and PEG-poly(ε-caprolactone) (PEG-PCL) and showed that the permeability, mechanical properties and the rate of degradation of the bi-layer membrane can be tuned by varying the length of the PEG as well as the character and length of the hydrophobic blocks [5,13]. However, the range of variation in the properties is rather limited, because there are constraints for the block copolymers to form Ps such as the hydrophilic block volume fraction and a low glass transition temperature (Tg) of the hydrophobic phase [4,14].

Significant efforts have been devoted to further control the membrane permeability of Ps by using block copolymers which are temperature sensitive, pH-responsive and which may be chemically or physically crosslinked [15–19]. An alternative approach is to modify the properties of the interior of the nanosized Ps for instance

* Corresponding author. Institute for Biomedical Technology and Technical Medicine (MIRA), Polymer Chemistry and Biomaterials Group, Faculty of Science and Technology, University of Twente, P.O. Box 217, 7500 AE, Enschede, The Netherlands. Tel.: +31 53 4892976/4892968; fax: +31 53 4892155.
E-mail address: j.feijen@tnw.utwente.nl (J. Feijen).

0168-3659/$ – see front matter © 2010 Elsevier B.V. All rights reserved.
doi:10.1016/j.jconrel.2010.06.002

by the introduction of a gel. Jesorka et al. have reported giant liposomes containing a PNIPAAm hydrogel, which were prepared by direct injection of a PNIPAAm solution into the liposomes [20,21]. It is obvious that this method is not practical for further applications.

The aim of this study is to develop a facile method for the introduction of a thermosensitive polymer solution, like PNIPAAm into Ps and to investigate the effect of the presence of the hydrogel inside the Ps on the release of a model compound. Monomethoxy poly (ethylene glycol)-b-poly(D,L-lactide), (mPEG-PDLLA) was used as a biodegradable and biocompatible amphiphilic block copolymer for the preparation of nanosized Ps. PDLLA can be degraded by hydrolysis [22,23] and PEG with a Mw less than 50,000 g/mol can be excreted by the kidneys [24]. Aqueous solutions of PNIPAAm have a sharp phase transition behavior and an LCST of 32 °C [25]. PNIPAAm has also been used as a component for the preparation of thermosensitive hydrogels, micelles, liposomes and Ps [15,26–30]. PNIPAAm containing Ps (N/Ps) were prepared by injecting a THF solution of the block copolymer and PNIPAAm into water. Gel containing Ps, further denoted as hydrosomes (Hs), were obtained by raising the temperature of N/Ps suspensions to 37 °C. After loading of N/Ps with drugs at room temperature and subsequent injection into the body, a prolonged delivery of the drug may be achieved because of the formation of a gel at 37 °C in the interior of the Ps (Fig. 1). The N/Ps and Hs were characterized by using dynamic light scattering (DLS), TEM and fluorescence studies. The release of the model compound, FITC-dextran (Mw 4000 g/mol), from Ps and Hs was evaluated to study the effect of the presence of a hydrogel inside Ps on its release rate.

2. Materials and methods

2.1. Materials

D,L-lactide (DLLA, Purac Biochem b.v., the Netherlands), *N*-isopropylacrylamide (NIPAAm, Aldrich, USA), and 2,2'-azobisisobutyronitrile (AIBN, Fluka, Switzerland) were recrystallized from toluene, hexane, and methanol, respectively. Monomethoxy poly (ethylene glycol) with a molecular weight of 5000 g/mol (mPEG, Fluka) was dried by dissolution in anhydrous toluene followed by azeotropic distillation under N_2. Stannous octoate (SnOct), fluorescamine and FITC-dextran (Mw 4000 g/mol) were obtained from Sigma (USA). Sodium tetraborate was supplied by Aldrich. Rhodamine B (RB), fluorescein isothiocyanate (FITC), 2-aminoethanethiol (AET), *N,N'*-dicyclohexylcarbodiimide (DCC), 4-di(methylamino)pyridine (DMAP) and uranyl acetate dihydrate were purchased from Fluka and used as received. Deionized water (DI water) was obtained from a Milli-Q water purification system (Millipore, France) and phosphate buffered saline (PBS, 0.01 M, pH 7.4, containing 0.02 wt.% NaN_3, B. Braun, USA) were used in the model drug release experiments.

2.2. Synthesis of (fluorescent-labeled) mPEG-PDLLA and PNIPAAm

mPEG-PDLLA was synthesized by ring-opening polymerization of DLLA using mPEG as an initiator (Fig. 2a). mPEG (0.50 g, 0.1 mmol), DLLA (4.11 g, 28.5 mmol), SnOct (0.04 g, 0.1 mmol) and toluene (16.5 ml) were charged in that order in a reaction vessel. The reaction was performed at 110 °C for 26 h under stirring. After cooling, a drop of HCl (37 wt.%) was added to the reaction mixture to hydrolyze the tin-oxygen bond. A sample was taken to determine the monomer conversion by ^{1}H NMR (Inova 300 MHz, Varian, USA). The copolymer was isolated by precipitation in methanol. After filtration and washing with methanol, the copolymer was dissolved in dichloromethane (DCM) and precipitated in diethyl ether. Subsequently, the polymer was isolated by filtration, washed several times with diethyl ether, and dried under vacuum. ^{1}H NMR analysis showed that the monomer conversion was 99% and that the Mn of the PDLLA block was 42,000 g/mol. Area integrations of the $\underline{CH}$–CH_3 peak (5.18 ppm) from PDLLA and the $\underline{CH_2}$–$\underline{CH_2}$–O peak (3.62 ppm) from mPEG were used for the calculation of the Mn.

Amine-terminated PNIPAAm (PNIPAAm-NH_2) was prepared by free radical polymerization of NIPAAm using AET as a chain transfer agent (Fig. 2b) as previously reported [29]. NIPAAm (11.30 g, 100 mmol), AIBN (0.14 g, 1 mmol) and AET (0.08 g, 1 mmol) were dissolved in methanol and the reaction mixture was heated at 60 °C for 20 h in a nitrogen atmosphere. The copolymer was recovered by precipitation into cold diethyl ether. This procedure was repeated twice and the polymer was dried in a vacuum oven. The LCST of an aqueous PNIPAAm solution (5 wt.%) was 32 °C as determined using a UV–visible spectrophotometer (CARY 300 Bio, Varian, USA). The Mn and Mw of PNIPAAm were analyzed by gel permeation chromatography (GPC) as 39,200 g/mol and 56,000 g/mol, respectively. The GPC was equipped with an RI detector (RI 2414 detector, Waters), Waters 515 pump and μStyragel columns (300×7.8 mm, 20 μm particle size, Waters). A DMF containing LiCl (0.1 M) was used as an eluent (flow rate 1 ml/min) and PNIPAAm (0.5 wt.%) was dissolved in the DMF solution for the GPC analysis (injection volume 30 μl). Poly(methyl methacrylate)s were used as calibration standards. The degree of functionalization of PNIPAAm with NH_2 was 96.0±4.7% ($n=3$, ave±std) as obtained by using the fluorescamine assay [31] using PEG diamine (IRIS Biotech, Germany Marktredwitz, Mn 23,100 g/mol) as a standard.

mPEG-PDLLA-RB was prepared by reacting mPEG-PDLLA (2.35 g, 0.05 mmol) with RB (0.03 g, 0.06 mmol) using DCC (0.01 g, 0.06 mmol) and DMAP (0.01 g, 0.06 mmol) in DCM (200 ml) at room temperature for 24 h (Fig. 2c) [32]. Residual urea was removed by repeated filtration until the solution was clear. Free RB was separated by ultrafiltration (cut-off 10,000 g/mol, Stirred Cells, Millipore co., USA). The PNIPAAm-NH_2 was labeled using FITC according to literature [33] as shown in Fig. 2d. FITC (0.06 g, 0.15 mmol) was dissolved in 0.1 M sodium tetraborate buffer (pH

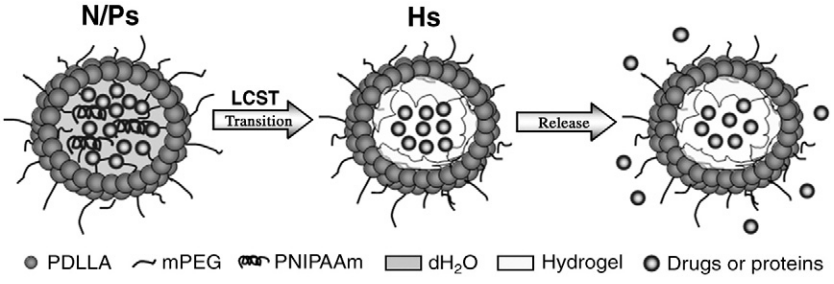

Fig. 1. Schematic 2D-cross sectional illustration of Ps and Hs in which the PNIPAAm solution present in the core phase separates and partially turns into a gel at the LCST of the internal PNIPAAm aqueous solution, influencing the release rate of incorporated agents.

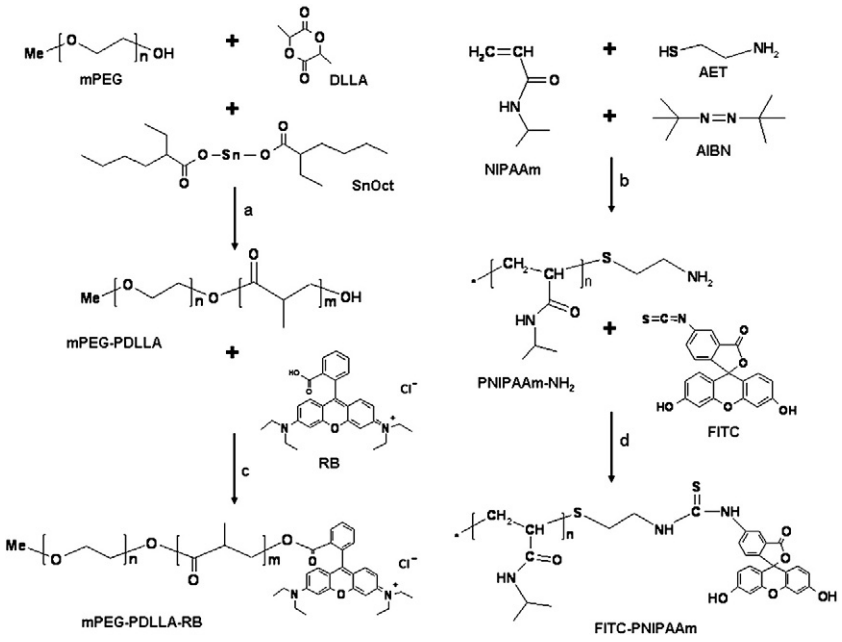

Fig. 2. Synthesis of (fluorescent-labeled) mPEG-PDLLA and PNIPAAm.

9.0, 150 ml), containing 10% (v/v) acetone. Aminated PNIPAAm (3.50 g, 0.10 mmol) was then dispersed in the resulting solution. The dispersion was stirred at room temperature for 6 h in the dark and free FITC was removed by ultrafiltration (cut-off 10,000 g/mol).

2.3. Preparation of N/Ps and FITC-N/Ps

Nano-sized N/Ps and FITC-N/Ps were prepared using the solvent injection method, allowing large-scale production of Ps [34]. In brief, the amphiphilic block copolymer (10 mg/ml) and PNIPAAm with or without the FITC label (50 mg/ml) were dissolved in THF (3 ml), and the THF solution was injected into an aqueous phase (50 ml). After 15 min without shaking, the mixture was gently inverted several times resulting in a turbid dispersion. To remove the organic solvent from the solution, the Ps dispersion was transferred into a dialysis bag (cut-off 50,000 g/mol, Spectra/Por, CA), which was placed in a 4 l flask with DI water for two days. DI water was replaced for at least 5 times. Subsequently, the dispersion was ultrafiltrated through a membrane (cut-off 100,000 g/mol, Ultracel Ultrafiltration Disc, Millipore, USA) for 5 h to remove non-encapsulated PNIPAAm. The purified solutions were concentrated 10 times during the ultrafiltration step. All procedures were carried out at room temperature.

2.4. DLS measurements and TEM

Size measurements of N/Ps and Hs were performed with a Zetasizer Nano ZS (Malvern Instruments, Malvern, UK) using a wavelength of 532 nm with a step-wise increase and subsequent decrease in temperature to examine the influence of the temperature on the size and a stability of the bi-layer membrane structure. The hydrodynamic radius (R_H) was measured by back-scattering at a detection angle of 173° using the Stokes–Einstein equation (Eq. (1)):

$$R_H = \frac{k_B T}{6\pi\eta D_0} \quad (1)$$

where k_B = Boltzmann constant, T = absolute temperature, η = solvent viscosity, D_0 = diffusion coefficient at infinite dilution. Bare Ps were prepared by the same method as mentioned above and used as a comparison. All samples were prepared by filtering the solutions through a 0.45 μm Millipore filter into cuvettes, which were subsequently mounted in a thermostated cell. The measurements were repeated five times.

Transmission electron microscopy (TEM, Philips CM30, Hillsboro, USA) was performed to elucidate the morphology and membrane thickness of Ps. For TEM, Ps dispersions were prepared by injecting a THF solution into an aqueous solution. A dispersion of empty Ps (2 μl) was placed on a 200 mesh carbon grid without using a staining agent and dried at room temperature. An N/Ps dispersion was kept at 37 °C to form Hs and 2 μl of the dispersion was deposited onto a 300 mesh carbon grid. After 30 s, Hs were stained with an uranyl acetate solution (2 wt.%) for 1 min. The excess solution was removed and the sample was dried at 37 °C.

2.5. Dual channel CLSM using FITC and RB

Fluorescence images were obtained by CLSM (LSM 510, Zeiss, Germany) equipped with a Zeiss Axiovert 100 M Inverted Microscope for Nomarski DIC and Epi-Fluorescence. FITC-N/RB-Ps were prepared using mPEG-PDLLA-RB and FITC-N by injecting a polymer solution (THF) into DI water. To observe the co-localization of the two different fluorescence markers, a double-illumination system consisting of an Ar laser and a He–Ne laser was employed for excitation of FITC and RB, respectively.

2.6. Fluorescence correlation spectroscopy

FCS has emerged as a sensitive technique operating at the level of single fluorescent molecules diffusing in and out of the confocal volume created by a focused laser beam. FCS of aqueous solutions of FITC, FITC-N and FITC-N/Ps was carried out at room temperature. Solutions of FITC and FITC-N were used as controls. FCS was carried out on a home-built set up [35], which can be briefly described as follows. Linearly polarized laser light with a wavelength of 488 nm was used to excite FITC. Light passed a dichroic mirror with a low-reflection/high-transmission (reflection <5%, transmission >95%) beam splitter and an objective. The fluorescence emission was collected by the same objective and >95% of fluorescent light passed through the dichroic mirror towards the detectors. The detection path consisting of a notch filter and folding mirrors were used to direct the

fluorescent light to an avalanche photodiode for FCS measurements or to a single-prism spectrometer equipped with a liquid nitrogen cooled charged-coupled device camera (SPEC-10 System, Princeton Instruments, Trenton, NJ) for spectral measurements. Spectral data were acquired frame by frame with the help of WINSPEC (Roper Scientific).

2.7. Fluorescence anisotropy measurements

For steady-state anisotropy measurements, a fluorescent sample was excited with linearly polarized light, yielding fluorescent light emission from the sample. FA data were determined with a fluorescence spectrophotometer (CARY Eclipse, Varian, USA) equipped with polarizers in the right-angle configuration and a temperature controller. The fluorescence anisotropy, $r(\lambda)$, was calculated directly from the uncorrected, polarized fluorescence, $I(\lambda)$, as follows:

$$r(\lambda) = \frac{I(\lambda)_{VV} - G(\lambda)I(\lambda)_{VH}}{I(\lambda)_{VV} + 2G(\lambda)I(\lambda)_{VH}}, \quad G(\lambda) = \frac{I(\lambda)_{HV}}{I(\lambda)_{HH}} \tag{2}$$

where the subscript-values refer to the horizontal or vertical settings of the excitation and emission polarizers, respectively. $G(\lambda)$ compensates for the wavelength-dependent, polarizing effects of the instrument. In FA, a higher value of r relates to a more restricted motion of the fluorophore during its fluorescence lifetime. In turbid media light scattering may also contribute to the measured anisotropy [36,37]. A solution of FITC-N/Ps was placed in a 1-mm-thin quartz cell and recorded at 25 °C (FITC-N/Ps) and 37 °C (FITC labeled Hs, FITC-Hs) with an excitation wavelength of 495 nm. Solutions of FITC and FITC-N were used as controls.

2.8. CLSM of giant FITC-N/Ps and FITC-Hs

To further study the formation of a PNIPAAm hydrogel in the Ps, giant FITC-N/Ps were prepared using FITC-N (50 mg/ml) and mPEG-PDLLA (10 mg/ml) by injecting solutions of these polymers in $CHCl_3$ (3 ml) as a water immiscible organic solvent into an aqueous solution (50 ml) and by evaporating $CHCl_3$ at ambient conditions for three days. To reveal the Ps with encapsulated FITC-N, the Ps dispersion was diluted 1:1 with DI water just before the CLSM analysis in order to decrease the fluorescence of the aqueous medium outside the Ps. For the CLSM studies, 1 ml of the FITC-N/Ps suspensions was introduced in homemade thin-glass-bottomed cuvettes, which were placed in the thermostated incubator at 25 °C and 37 °C (TC-202A Bipolar Temperature Controller, Harvard Apparatus, USA).

2.9. Release of FD from Ps, N/Ps and Hs

FITC-dextran (FD)-loaded N/Ps (FD-N/Ps) were prepared by injecting the appropriate THF solution into DI water as previously mentioned. In this case, FD (500 mg/ml) was added to a DI water solution (50 ml) while PNIPAAm (50 mg/ml) and mPEG-PDLLA (10 mg/ml) were dissolved in THF (3 ml). Free FD and free PNIPAAm were removed by ultrafiltration (cut-off 100,000 g/mol) for 24 h at room temperature. To determine the amount of loaded FD, Ps were solubilized using Triton X-100 [38]. After adding Triton X-100 to the Ps dispersion with a final concentration of 2 wt.%, the mixture was heated for 3 h at 80 °C. The release of FD both at 25 °C and 37 °C from suspensions of Ps placed in a microdialysis system was monitored by periodic withdrawals of PBS samples. The release of FD from Ps filled with either gel or sol was studied by placing a dispersion of Ps (1 ml) into a dialysis bag (cut-off 100,000 g/mol) and immersing the bag into a large vial containing 29 ml of PBS. The experiments were carried out in three-fold. The release of free FD from an empty dialysis bag was also measured to confirm that the dialysis membrane was not rate controlling in the release experiment. At appropriate times, 1 ml of the release medium was collected from the vials and the medium was replaced by fresh PBS. Concentrations of released FD were determined by fluorescence spectroscopy (Safire^2, Tecan, Canada) at an emission wavelength of 516 nm and an excitation wavelength of 495 nm. In this way, the loaded amounts of FD as well as the release kinetics were obtained. The stability of the FD-containing Hs (FD-Hs) during drug delivery was evaluated by measuring the size, count rate and polydispersity index (PDI) by DLS at 37 °C. FD-Hs suspensions were incubated using the same method and conditions as used for FD release experiments. Data were collected at different incubation times.

3. Results and discussion

3.1. Formation of nanosized Ps, N/Ps and Hs

Drug delivery systems based on self-assembled carriers have received widespread interest since the 1980s [39]. The design and evaluation of micelles and liposomes as drug delivery carriers have received a lot of attention. A drawback of these systems is that they often accumulate in the liver and spleen via a rapid uptake by the RES. Moreover these systems are often not stable in the circulation [3]. In contrast, Ps can be designed to have a stable membrane and a relatively bioinert surface. The uptake of Ps with a size lower than 200 nm by the RES can be reduced, while extravasation from leaky capillaries is enhanced [40].

Ps can be prepared by sonication of an aqueous copolymer dispersion, hydration of a copolymer film and rehydration using various solvent compositions (organic solvent/water mixtures) [6]. However, these techniques have substantial shortcomings, including rather complicated preparation and filtration procedures. In this study, Ps containing PNIPAAm with an average diameter of 163 nm (25 °C) and a narrow size distribution (Fig. 3) were prepared by a simple solvent injection method [41] using a THF solution of the copolymer and PNIPAAm. The corresponding Ps without PNIPAAm had a diameter of 120 nm at 25 °C (Fig. 3a). The larger size of N/Ps as compared to the Ps is possibly due to an increase of the interfacial free

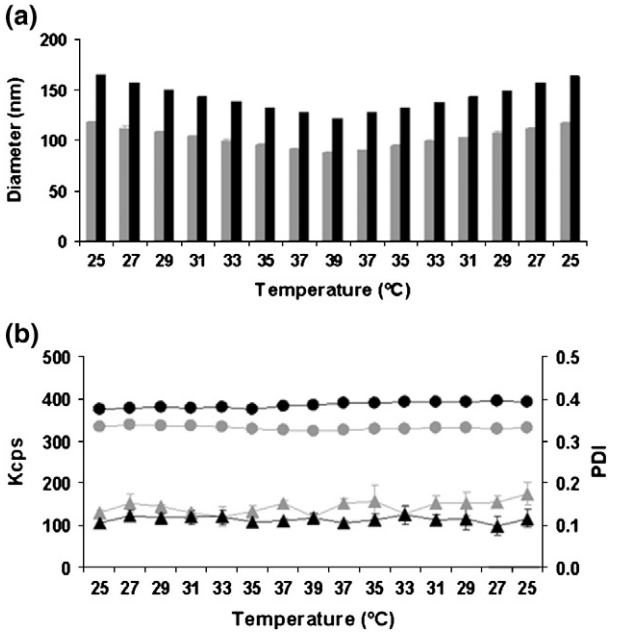

Fig. 3. DLS measurements of Ps prepared with or without PNIPAAm as a function of temperature (heating and cooling in a step-wise manner). Ps (●, ▲ and gray bars), N/Ps and Hs (●, ▲ and black bars). Diameter (gray and black bars), kilo count per second (Kcps) (● and ●) and polydispersity index (PDI) (▲ and ▲). Measurements were performed 30 times and averaged. Error bars represent standard deviations.

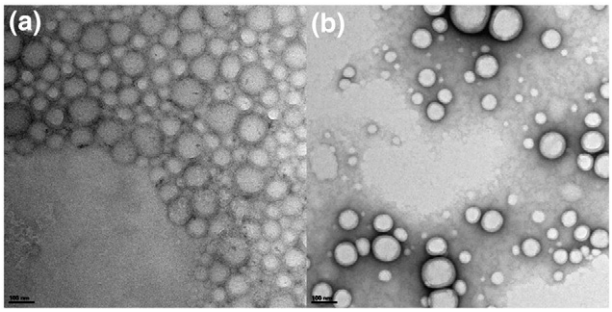

Fig. 4. TEM images of empty Ps (a) and nanosized Hs (b) on carbon grids. (a): A dispersion of empty Ps was placed on a 200 mesh normal carbon grid without using a staining agent and dried at room temperature. (b): A drop of the pre-equilibrated Hs dispersion at 37 °C was deposited onto a 300 mesh porous carbon grid and stained by uranyl acetate. Size bars represent 100 nm.

energy at the interior surface of the N/Ps. Both the size of the N/Ps and Ps decrease with increasing the temperature to 37 °C and the original sizes were obtained again by cooling to 25 °C. These effects may be due to partial dehydration of ethylene oxide groups in the PEG blocks with increasing temperature [42]. DLS measurements show that the Kcps and PDI of the N/Ps are not changing during the temperature cycle. Based on these data and the thermoreversible changes in size of the N/Ps, it can be concluded that the expected hydrogel formation of the PNIPAAm solution inside the Ps did not disrupt the membrane of the Ps (Fig. 3b).

TEM was performed to directly visualize the morphology and to evaluate the membrane thickness of Ps. Fig. 4a shows a TEM image of empty Ps. Fig. 4b represents a TEM image of Hs, which were deposited onto a carbon grid at 37 °C after pre-equilibration at 37 °C. It can be seen that the Hs are spherical nanocapsules after the phase transition of the incorporated PNIPAAm solution. Vesicles with a diameter varying from 50 to 150 nm can be observed, which corresponds well with the size distribution obtained from the DLS analysis as shown in Fig. 3a. The membrane thickness was about 15 nm for both Ps and Hs, and the thickness was not dependent on the size of the vesicles.

3.2. Co-localization of PNIPAAm and Ps: dual fluorescence CLSM

To prove that PNIPAAm was co-localized with Ps, FITC-N and RB labeled Ps (RB-Ps) were used for dual fluorescence CLSM. Fig. 5 shows images of the green fluorescence of the FITC label, the red fluorescence of the RB label and the combination of both fluorescent labels. The combined image indicates that FITC-N and RB-Ps were co-localized.

3.3. Co-localization of PNIPAAm and Ps: fluorescence correlation spectroscopy

To further investigate the association of PNIPAAm and Ps, fluorescence correlation spectroscopy (FCS) measurements were carried out on Ps containing FITC-N at room temperature. FCS of the free FITC solution and the FITC-N solution were used as controls. Fluorescence intensity fluctuations due to the diffusion of fluorescent molecules in and out of the excitation volume were monitored. Fig. 6a shows intense bursts of fluorescence from FITC-N/Ps. Long residence times (8.82 ± 7.71 ms) are associated with the relatively slow diffusion of Ps with co-localized FITC-N (Table 1). FITC-N had a short residence time, which reflects a relatively fast diffusion of the FITC coupled PNIPAAm molecules (Fig. 6c). As expected, the diffusion of free FITC was even faster (residence time of 0.04 ± 0.01 ms) than that of FITC-N in which FITC was coupled to a relatively high molecular weight PNIPAAm polymer (Fig. 6b). Non-labeled PNIPAAm and Ps were used as controls (Fig. 6d and e). These results confirm again that PNIPAAm is co-localized with Ps.

3.4. Internal PNIPAAm hydrogel formation: steady state fluorescence anisotropy

To get information on the sol-gel transition of internalized PNIPAAm solution with Ps, steady state FA measurements on FITC-N/Ps and -Hs were performed and compared with free FITC and FITC-N. The r values of solutions of these compounds and Ps dispersions were recorded as a function of the wavelength (Fig. 7). At $\lambda < 520$ nm, the anisotropy measurements are affected by light scattering. Average r values were calculated from the measurements at $\lambda > 520$ nm and given in Table 2. Aqueous solutions (10 μM) of both free FITC at 25 °C and 37 °C, and FITC-N at 25 °C showed a low r value of ~0.012 (Fig. 7a and b) reflecting a high rotational freedom of FITC. The r value of FITC-N/Ps was 7 times higher than that of free FITC-N and free FITC indicating that the FITC label of PNIPAAm internalized in the Ps was strongly hindered in its rotational motion. A possible local high concentration of the PNIPAAm solution in the Ps could also contribute to a decrease of the rotational freedom of FITC. However, at the moment it is not possible to calculate the exact PNIPAAm concentration in the Ps. Based on the r values of FITC-N and free FITC, the translational and rotational diffusion of the label were similar at 25 °C.

When the temperature was increased to 37 °C, an increase of r was observed for the FITC-N solution. This was a result of the coil to globular transition of PNIPAAm and possible subsequent self-aggregation of PNIPAAm chains as a result of intramolecular dehydration [43]. We also noted an increase in the r below a wavelength of 520 nm due to a slight increase in (polarized) light scattering. Upon increasing the temperature from 25 °C to 37 °C, the r value was increased significantly from 0.096 to 0.148 (Fig. 7c). These results demonstrate that the PNIPAAm concentration of the internal solution was high enough to form a hydrogel, which suppresses the rotational freedom of the FITC label.

3.5. Internal PNIPAAm hydrogel formation: CLSM using giant N/Ps and Hs

In order to establish the presence of a PNIPAAm hydrogel and its formation after phase separation in Ps, giant FITC-N/Ps and -Hs were

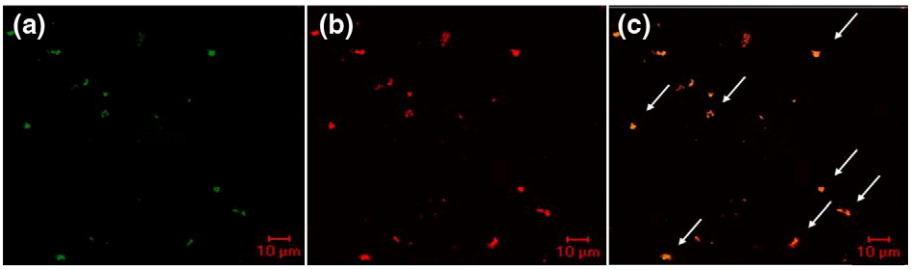

Fig. 5. Dual fluorescence CLSM images of FITC-N and RB-Ps prepared by the injection of a THF solution of labeled polymers into water. FITC and RB were illuminated using two different laser channels resulting in a green color (a) and a red color (b), respectively. The combined image of panel (a) and panel (b) is represented in panel (c). Size bars are 10 μm and arrows mark the co-localization of FITC-N and RB-Ps. (For interpretation of the references to color in this figure legend, the reader is referred to the web version of this article.)

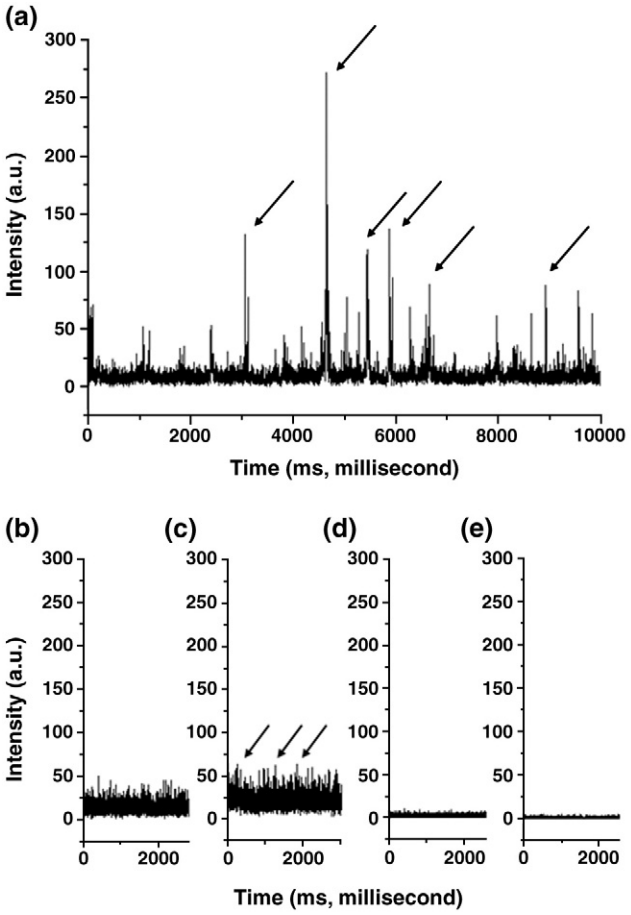

Fig. 6. FCS of FITC, FITC-N and FITC-N/Ps at 25 °C. Non-labeled Ps and PNIPAAm were used as controls. (a) FITC-N/Ps, (b) free FITC (10 μM), (c) FITC-N (10 μM), (d) Ps and (e) PNIPAAm. Arrows represent fluorescence bursts indicating the passage of fluorescent molecules in and out of the laser detection area.

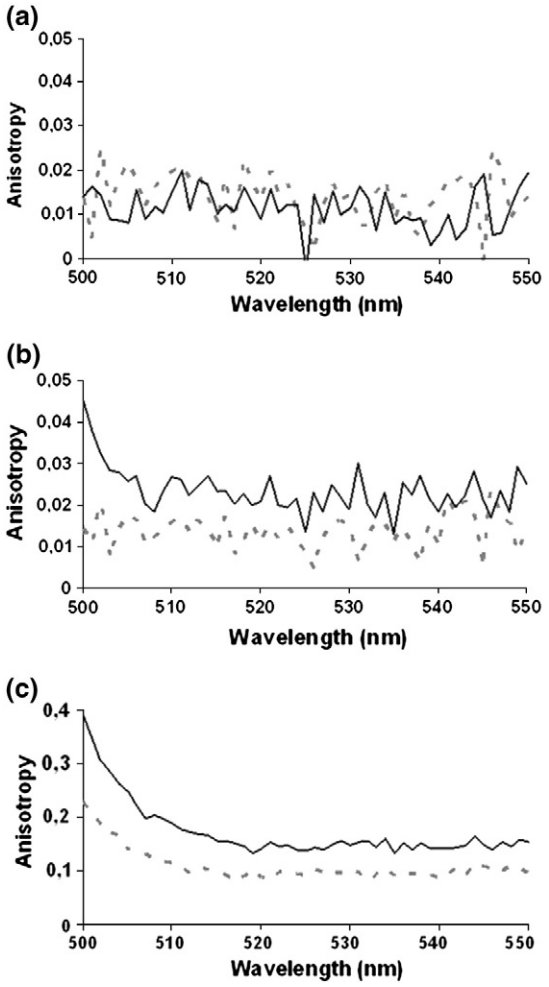

Fig. 7. Temperature-dependent fluorescent anisotropy (r) values of FITC, FITC-N and FITC-N in Ps at 25 °C (gray dashed lines) and 37 °C (black solid lines). (a) free FITC (10 μM), (b) FITC-N (10 μM), and (c) FITC-N/Ps (25 °C) and -Hs (37 °C).

used for CLSM. The FITC-N/Ps with a diameter of 5–10 μm were prepared using $CHCl_3$ instead of THF as a organic phase. The gel formation and phase separation of the PNIPAAm solution in the giant Hs could be observed using CLSM combining both fluorescence — and bright field microscopy. Fig. 8c provides evidence of the presence of FITC-N inside the Ps below the LCST of the FITC-N solution. Above this temperature, phase separation of the solution took place leading to a PNIPAAm hydrogel and an aqueous phase (Fig. 8f). It should be noted that a solution of PNIPAAm can phase-separate into an aqueous phase and a gel phase with a volume of 10–20% of the total volume when the concentration of the initial PNIPAAm solution is high enough to form a hydrogel [44,45]. Phase separation is further corroborated by the data on the anisotropy measurements of the Ps containing FITC-N. It was also observed that the PNIPAAm hydrogel was preferentially localized in the vicinity of the membrane of giant Ps rather than in the center of the cavity (Fig. 8g). Finally, Fig. 8b and e confirms the hollow sphere structure before and after the internal hydrogel formation, respectively, indicating that the membrane of the giant Ps is not disrupted during the sol-gel transition. Disruption of the membrane of nanosized N/Ps during the phase transition also did not take place according to the DLS results (Fig. 3).

Table 1
Residence times of FITC, FITC-N and FITC-N/Ps obtained by FCS.

	Free FITC[a]	FITC-N[a]	FITC-N/Ps
Residence time (ms)	0.04 ± 0.01	0.08 ± 0.03	8.82 ± 7.71

[a] 10 μM aqueous solution.

3.6. Release of FITC-dextran (FD) from Ps, N/Ps and Hs

FD with a molecular weight of 4000 was used as a model compound to investigate the release kinetics from Ps at different temperatures. Fig. 9a and b represent the release profiles of FD from different vesicles at 25 °C and 37 °C placed in a dialysis bag. The release of FD from the empty dialysis membrane was fast and did hardly influence the release data for the vesicles. All release profiles for the vesicles showed an initial burst of 10–20% followed by a gradual decrease of the release rate (Fig. 9b).

Fig. 9a shows that FD was completely released from the Hs at 37 °C after a month, while the release from Ps at 37 °C was already completed after 6 days. The difference in release rates has to be due to the presence of a hydrogel in the Hs. As discussed before, the PNIPAAm solution in the vesicles separates in two phases above the LCST forming a gel and an aqueous solution. Based on distribution studies of FD in a phase separated PNIPAAm system, it was estimated that about 80% of encapsulated FD was in the aqueous phase and 20%

Table 2
Average r values monitored from 520 to 550 nm.

	Free FITC[a]	FITC-N[a]	FITC-N/Ps (25 °C) and -Hs (37 °C)
25 °C	0.013 ± 0.006	0.013 ± 0.005	0.096 ± 0.007
37 °C	0.011 ± 0.005	0.022 ± 0.004	0.148 ± 0.007

[a] 10 μM aqueous solution.

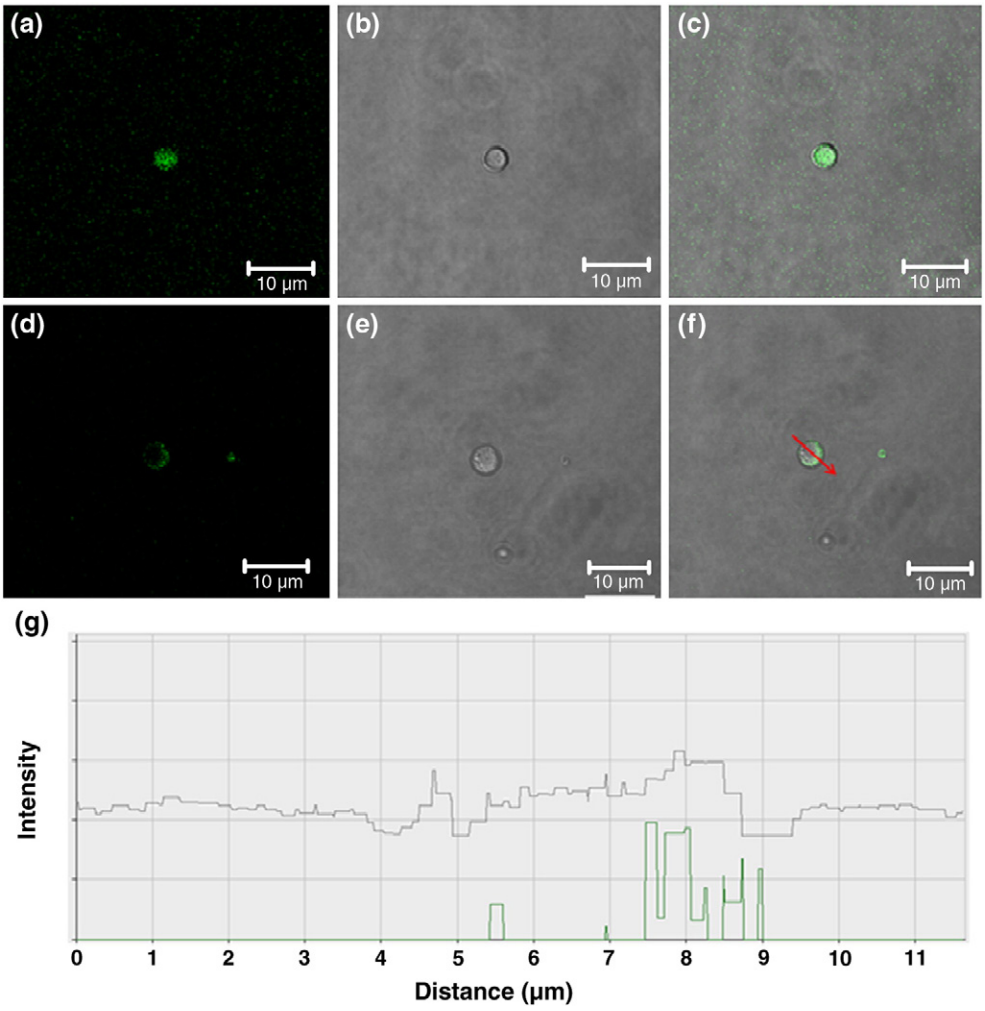

Fig. 8. FITC-N containing giant Ps and Hs were imaged using CLSM at different temperatures to visualize internal gelation of the FITC-N solution. Giant FITC-N/Ps were prepared by injection of a chloroform solution of the copolymer and FITC-N into water. Fluorescence images (a and d), bright field images (b and e) and combined images (c and f) were taken at two different temperatures (upper panels: FITC-N/Ps at 25 °C and lower panels: FITC-Hs at 37 °C). White light and fluorescence intensities were scanned as indicated by a red arrow in (f). Gray lines and green lines show white light and fluorescence profiles, respectively (g). Size bars represent 10 μm. (For interpretation of the references to color in this figure legend, the reader is referred to the web version of this article.)

in the gel phase (data not shown). As shown before, the hydrogel was located very close to the membrane of the Hs. Therefore, the hydrogel forms an extra barrier for release of the FD and also limits the available free membrane area for permeation of FD from the aqueous solution inside the Hs. A possible interaction between the internal PEG chains and PNIPAAm chains may explain the localization of the gel in conjunction with the membrane of the Ps. This is further supported by the work of Polozova and Winnik [46] who concluded that the amide groups of PNIPAAm may form hydrogen bonds with ethylene oxide units. This not only can explain the image shown in Fig.8f, but also the sustained FD release from Hs at 37 °C. Both Hs and empty Ps show a more rapid release of FD at 37 °C than at 25 °C due to an increase in the membrane permeability. Both N/Ps and empty Ps have similar FD release profiles at 25 °C, indicating that the presence of a PNIPAAm solution in Ps did not lead to a prolonged release of FD. It can also be seen that at 37 °C the release of FD from Hs is faster than the release from N/Ps at 25 °C. Apparently, the increase of the permeability of the membrane with temperature has a stronger effect on the release than the formation of the membrane associated hydrogel.

In order to understand a possible influence of the degradation of the Ps membrane in time on the release of FD from Hs, DLS measurements of the FD-Hs were carried out at different time points and the size distribution, Kcps and PDI were monitored. FD-Hs showed an excellent stability during 20 days based on their narrow and unimodal size distribution. After 20 days of incubation, Hs formed aggregates possibly facilitated by the presence of PNIPAAm (Fig. 9c). This can be explained by gradual hydrolysis of the PDLLA block, which eventually leads to destabilization of the bi-layer. Initially, chains with comparatively short hydrophobic blocks will tend to segregate and ultimately may induce hydrophilic pores in the membrane [13]. Therefore, the accelerated release rate of FD from Hs after 20 days at 37 °C can be explained by the gradual degradation of the PDLA blocks of the copolymer forming the membrane.

4. Conclusions

Novel bi-layer-enclosed nano-compartments containing a thermosensitive hydrogel, further named hydrosomes, were developed and characterized. This new controlled release system is composed of polymersomes (Ps) with a biodegradable mPEG-PDLLA membrane containing a PNIPAAm solution inside the reservoir at 25 °C. Above the LCST of the PNIPAAm solution in the Ps, phase separation takes place, and a hydrogel and an aqueous phase are formed. The presence of the PNIPAAm solution in the Ps was shown by dual fluorescence CLSM, FCS, FA and CLSM of PNIPAAm containing giant Ps. FITC-dextran (FD) with a molecular weight of 4000 was released over a period of 4 weeks from Ps at 37 °C with a low initial burst, while the release from Ps not containing PNIPAAm was completed in 6 days. These

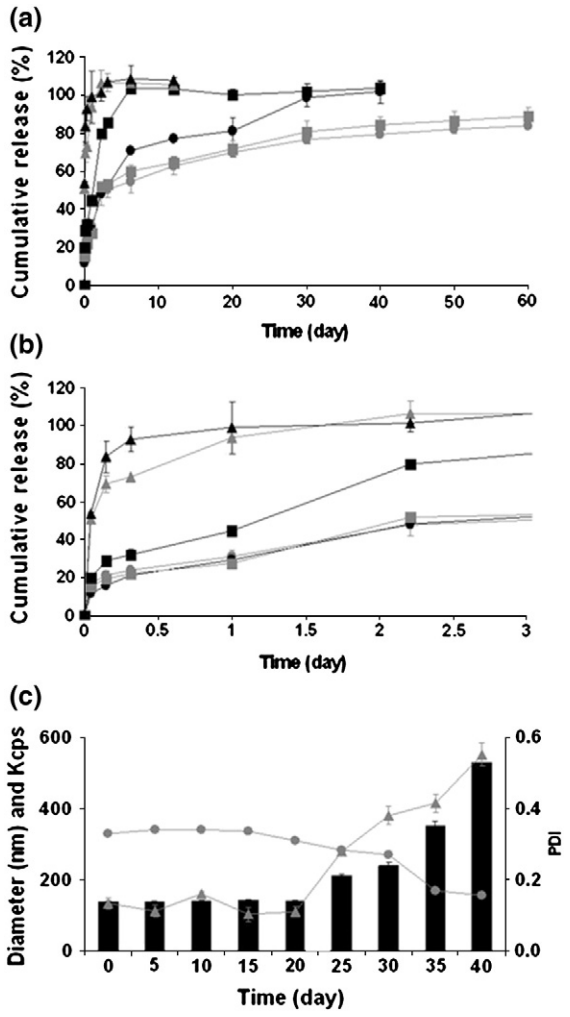

Fig. 9. FD release from Ps at 25 °C and 37 °C, N/Ps and Hs measured with fluorescence spectroscopy. (a) FD release from the dialysis bag at 25 °C (▲) and at 37 °C (▲), FD release from Ps at 25 °C (■) and at 37 °C (■), and from N/Ps (25 °C, ●) and from Hs (37 °C, ●). At different time intervals, 1 ml of the release medium was collected and analyzed by fluorescence spectroscopy. The experiments were carried out in triplicate. (b) FD release data for the first 3 days (enlargement of Fig. 9a). The stability of the FD-Hs vesicles at 37 °C was investigated over a period of 60 days by analyzing the samples for the release data with DLS. (c) DLS data of FD-Hs as a function of time. Diameter (black bars), Kcps (●) and PDI (▲). DLS measurements were performed 30 times per sample. The data given are mean values and the error bars are the standard deviations of the mean.

results are explained by the formation of a membrane associated PNIPAAm hydrogel layer in the hydrosomes (Hs), which strongly reduces the release rate of FD. In our current program, we further focus on the introduction of stimuli-sensitive nanogels in Ps to effectively control the site specific release of drugs and proteins.

Acknowledgements

The authors thank Mark Smithers (MESA$^+$, University of Twente) for TEM measurements and Clemens Padberg (MTP, University of Twente) for the GPC analysis.

References

[1] P.B. Malafaya, G.A. Silva, E.T. Baran, R.L. Reis, Drug delivery therapies I — general trends and its importance on bone tissue engineering applications, Curr. Opin. Solid State Mater. Sci. 6 (4) (2002) 283–295.
[2] V.R. Sinha, A. Trehan, Biodegradable microspheres for parenteral delivery, Crit. Rev. Ther. Drug Carrier Syst. 22 (6) (2005) 535–602.
[3] L.Y. Qiu, Y.H. Bae, Polymer architecture and drug delivery, Pharm. Res. 23 (1) (2006) 1–30.
[4] B.M. Discher, D.A. Hammer, F.S. Bates, D.E. Discher, Polymer vesicles in various media, Curr. Opin. Colloid Interface Sci. 5 (1–2) (2000) 125–131.
[5] H. Bermudez, A.K. Brannan, D.A. Hammer, F.S. Bates, D.E. Discher, Molecular weight dependence of polymersome membrane structure, elasticity, and stability, Macromolecules 35 (21) (2002) 8203–8208.
[6] J.C.M. Lee, H. Bermudez, B.M. Discher, M.A. Sheehan, Y.Y. Won, F.S. Bates, D.E. Discher, Preparation, stability, and in vitro performance of vesicles made with diblock copolymers, Biotechnol. Bioeng. 73 (2) (2001) 135–145.
[7] P.J. Photos, L. Bacakova, B. Discher, F.S. Bates, D.E. Discher, Polymer vesicles in vivo: correlations with PEG molecular weight, J. Control. Release 90 (3) (2003) 323–334.
[8] R. Gref, Y. Minamitake, M.T. Peracchia, V. Trubetskoy, V. Torchilin, R. Langer, Biodegradable long-circulating polymeric nanospheres, Science 263 (5153) (1994) 1600–1603.
[9] S. Stolnik, L. Illum, S.S. Davis, Long Circulating Microparticulate Drug Carriers, Adv. Drug Deliv. Rev. 16 (2–3) (1995) 195–214.
[10] S.I. Jeon, J.H. Lee, J.D. Andrade, P.G. Degennes, Protein surface interactions in the presence of polyethylene oxide. 1. Simplified theory, J. Colloid Interface Sci. 142 (1) (1991) 149–158.
[11] S.I. Jeon, J.D. Andrade, Protein surface interactions in the presence of polyethylene oxide. 2. Effect of protein size, J. Colloid Interface Sci. 142 (1) (1991) 159–166.
[12] K.D. Park, Y.S. Kim, D.K. Han, Y.H. Kim, E.H.B. Lee, H. Suh, K.S. Choi, Bacterial adhesion on PEG modified polyurethane surfaces, Biomaterials 19 (7–9) (1998) 851–859.
[13] F. Ahmed, P.J. Photos, D.E. Discher, Polymersomes as viral capsid mimics, Drug Dev. Res. 67 (1) (2006) 4–14.
[14] A. Mecke, C. Dittrich, W. Meier, Biomimetic membranes designed from amphiphilic block copolymers, Soft Matter 2 (9) (2006) 751–759.
[15] L.Y. Chu, S.H. Park, T. Yamaguchi, S. Nakao, Preparation of thermo-responsive core-shell microcapsules with a porous membrane and poly(N-isopropylacrylamide) gates, J. Membr. Sci. 192 (1–2) (2001) 27–39.
[16] H.W. Duan, M. Kuang, G. Zhang, D.Y. Wang, D.G. Kurth, H. Mohwald, pH-responsive capsules derived from nanocrystal templating, Langmuir 21 (24) (2005) 11495–11499.
[17] F.T. Liu, A. Eisenberg, Preparation and pH triggered inversion of vesicles from poly (acrylic acid)-block-polystyrene-block-poly(4-vinyl pyridine), J. Am. Chem. Soc. 125 (49) (2003) 15059–15064.
[18] F.H. Meng, Z.Y. Zhong, J. Feijen, Stimuli-responsive polymersomes for programmed drug delivery, Biomacromolecules 10 (2) (2009) 197–209.
[19] C. Nardin, T. Hirt, J. Leukel, W. Meier, Polymerized ABA triblock copolymer vesicles, Langmuir 16 (3) (2000) 1035–1041.
[20] A. Jesorka, M. Markstrom, M. Karlsson, O. Orwar, Controlled hydrogel formation in the internal compartment of giant unilamellar vesicles, J. Phys. Chem. B 109 (31) (2005) 14759–14763.
[21] A. Jesorka, M. Markstrom, O. Orwar, Controlling the internal structure of giant unilamellar vesicles by means of reversible temperature dependent sol-gel transition of internalized poly (N-isopropyl acrylamide), Langmuir 21 (4) (2005) 1230–1237.
[22] J.M. Anderson, M.S. Shive, Biodegradation and biocompatibility of PLA and PLGA microspheres, Adv. Drug Deliv. Rev. 28 (1) (1997) 5–24.
[23] I. Grizzi, H. Garreau, S. Li, M. Vert, Hydrolytic degradation of devices based on poly (DI-lactic acid) size-dependence, Biomaterials 16 (4) (1995) 305–311.
[24] T. Yamaoka, Y. Tabata, Y. Ikada, Distribution and tissue uptake of poly(ethylene glycol) with different molecular-weights after intravenous administration to mice, J. Pharm. Sci. 83 (4) (1994) 601–606.
[25] C. Boutris, E.G. Chatzi, C. Kiparissides, Characterization of the LCST behaviour of aqueous poly(N-isopropylacrylamide) solutions by thermal and cloud point techniques, Polymer 38 (10) (1997) 2567–2570.
[26] S. Cammas, K. Suzuki, C. Sone, Y. Sakurai, K. Kataoka, T. Okano, Thermo-responsive polymer nanoparticles with a core-shell micelle structure as site-specific drug carriers, J. Control. Release 48 (2–3) (1997) 157–164.
[27] F. Kohori, K. Sakai, T. Aoyagi, M. Yokoyama, Y. Sakurai, T. Okano, Preparation and characterization of thermally responsive block copolymer micelles comprising poly(N-isopropylacrylamide-b-DL-lactide), J. Control. Release 55 (1) (1998) 87–98.
[28] K. Kono, A. Henmi, H. Yamashita, H. Hayashi, T. Takagishi, Improvement of temperature-sensitivity of poly(N-isopropylacrylamide)-modified liposomes, J. Control. Release 59 (1) (1999) 63–75.
[29] D.E. Meyer, B.C. Shin, G.A. Kong, M.W. Dewhirst, A. Chilkoti, Drug targeting using thermally responsive polymers and local hyperthermia, J. Control. Release 74 (1–3) (2001) 213–224.
[30] S.H. Qin, Y. Geng, D.E. Discher, S. Yang, Temperature-controlled assembly and release from polymer vesicles of poly(ethylene oxide)-block-poly(N-isopropylacrylamide), Adv. Mater. 18 (21) (2006) 2905–2909.
[31] S. Udenfrie, S. Stein, P. Bohlen, W. Dairman, Fluorescamine — reagent for assay of amino-acids, peptides, proteins, and primary amines in picomole range, Science 178 (4063) (1972) 871–872.
[32] H.A. Klok, J.J. Hwang, S.N. Iyer, S.I. Stupp, Cholesteryl-(L-lactic acid)((n)over-bar) building blocks for self-assembling biomaterials, Macromolecules 35 (3) (2002) 746–759.
[33] B. Elmas, M. Tuncel, G. Yalcin, S. Senel, A. Tuncel, Synthesis of uniform, fluorescent poly(glycidyl methacrylate) based particles and their characterization by confocal laser scanning microscopy, Colloid Surf. A-Physicochem. Eng. Aspects 269 (1–3) (2005) 125–134.

[34] M.E. Yildiz, R.K. Prud'homme, I. Robb, D.H. Adamson, Formation and characterization of polymersomes made by a solvent injection method, Polym. Adv. Technol. 18 (6) (2007) 427–432.
[35] D. Zhang, H. Lans, W. Vermeulen, A. Lenferink, C. Otto, Quantitative fluorescence correlation spectroscopy reveals a 1000-fold increase in lifetime of protein functionality, Biophys. J. 95 (7) (2008) 3439–3446.
[36] G. Hungerford, A.L.F. Baptista, P.J.G. Coutinho, E.M.S. Castanheira, M.E.C.D.R. Oliveira, Interaction of DODAB with neutral phospholipids and cholesterol studied using fluorescence anisotropy, J. Photochem. Photobiol. A-Chem. 181 (1) (2006) 99–105.
[37] B.R. Lentz, Use of fluorescent-probes to monitor molecular order and motions within liposome bilayers, Chem. Phys. Lipids 64 (1–3) (1993) 99–116.
[38] V. Pata, F. Ahmed, D.E. Discher, N. Dan, Membrane solubilization by detergent: resistance conferred by thickness, Langmuir 20 (10) (2004) 3888–3893.
[39] H. Bader, H. Ringsdorf, B. Schmidt, Watersoluble Polymers in Medicine, Angewandte Makromolekulare Chemie 123 (Aug. 1984) 457–485.
[40] A. Lavasanifar, J. Samuel, G.S. Kwon, Poly(ethylene oxide)-block-poly(L-amino acid) micelles for drug delivery, Adv. Drug Deliv. Rev. 54 (2) (2002) 169–190.
[41] F.H. Meng, G.H.M. Engbers, J. Feijen, Biodegradable polymersomes as a basis for artificial cells: encapsulation, release and targeting, J. Control. Release 101 (1–3) (2005) 187–198.
[42] S.Y. Park, B.R. Han, K.M. Na, D.K. Han, S.C. Kim, Micellization and gelation of aqueous solutions of star-shaped PLLA-PEO block copolymers, Macromolecules 36 (11) (2003) 4115–4124.
[43] R. Walter, J. Ricka, C. Quellet, R. Nyffenegger, T. Binkert, Coil-globule transition of poly(N-isopropylacrylamide): a study of polymer-surfactant association, Macromolecules 29 (11) (1996) 4019–4028.
[44] E. Ruel-Gariepy, J.C. Leroux, In situ-forming hydrogels — review of temperature-sensitive systems, Eur. J. Pharm. Biopharm. 58 (2) (2004) 409–426.
[45] Y. Suzuki, K. Tomonaga, M. Kumazaki, I. Nishio, Change in phase transition behavior of an NIPA gel induced by solvent composition: hydrophobic effect, Polym. Gels Netw. 4 (2) (1996) 129–142.
[46] A. Polozova, F.M. Winnik, Contribution of hydrogen bonding to the association of liposomes and an anionic hydrophobically modified poly(N-isopropylacrylamide), Langmuir 15 (12) (1999) 4222–4229.